Available online at www.sciencedirect.com
ScienceDirect
International Journal of Solids and Structures 44 (2007) 7323–7339
INTERNATIONAL JOURNAL OF SOLIDS AND STRUCTURES
www.elsevier.com/locate/ijsolstr

Transient responses of repeated impact of a beam against a stop

X.C. Yin [a,*], Y. Qin [b], H. Zou [a]

[a] Department of Mechanics and Engineering Science, Nanjing University of Science and Technology, Nanjing 210014, PR China
[b] Department of Design, Manufacture and Engineering Management, University of Strathclyde, Glasgow G1 1XJ, UK

Received 12 July 2006; received in revised form 27 February 2007
Available online 21 April 2007

Abstract

The transient behavior of a cantilever beam, driven by periodic force and repeated impacting against a rod-like stop, is the subject of this investigation. As impact and separation phase take place alternately, the transient waves induced either by impacts or by separations will travel in more complicated ways. Thus the transient responses of both the beam and the rod during repeated impact become an important issue. In both impact phase and separation phase, the transient wave propagations are solved by the expansion of transient wave functions in a series of Eigenfunctions (wave modes). From the solutions, the answer of impact force is derived directly, so that the divergence problem, encountered in solving impact force numerically by a strongly non-linear equation coupled the unknown impact force with motions, has been avoided. Numerical results show the convergence of the time-step size and truncation number of wave modes in the calculations of impact force by the present method. As the transient wave effect is considered, the numerical results can show several transient phenomena involving the propagation of transient impact-induced waves, sub-impact phases, long-term impact motion, chatter, sticking motion, synchronous impact, non-synchronous impact (including asynchronous impact) and impact loss.

Keywords: Repeated impact; Transient response; Wave; Beam; Rod

1. Introduction

The phenomenon of repeated impact is of great interest in science and engineering (Goldsmith, 1960; Babitsky, 1978). Some industrial devices utilize repeated impact as driving forces, for example, electrical and pneumatic hammers, vibratory feeders and shakers, impact bin vibrators, pile drivers, percussive-rotary drills, printers, impact dampers, and etc. However, in a large number of industrial systems, there is encountered extensively undesirable repeated impact that causes large vibrations, wear, impact noise and failure. A long list may include these familiar systems: switches and relays (Peek and Wagar, 1955), valves (Santos et al., 1991; Lee, 2004; Wang and Kim, 1996), gear pairs (Kahraman and Blankenship, 1997; Theodossiades and Natsiavas, 2001), heat exchangers (Knudsen and Massih, 2000), planar and spatial

* Corresponding author. Tel.: +86 25 8431 55 90.
E-mail address: yinxiaochun2000@yahoo.com.cn (X.C. Yin).

0020-7683/$ - see front matter © 2007 Elsevier Ltd. All rights reserved.
doi:10.1016/j.ijsolstr.2007.04.009

mechanisms (Dubowsky and Freudenstein, 1971; Oppenheimer and Dubowsky, 2003), machine tools (Leine et al., 2002), robot arms and mechanical manipulators (Yigit et al., 1990), wheel/rail systems (Wu and Thompson, 2004), bridges with expansion joints (Maragakis and Jennings, 1987) and adjacent buildings pounded during earthquakes (Lin and Weng, 2001). Many impacting components are beam-like components and may impact against a stop. The stop structure may be a massive compact component (Peek and Wagar, 1955; Santos et al., 1991; Lee, 2004; Knudsen and Massih, 2000; Leine et al., 2002; Yigit et al., 1990; Wu and Thompson, 2004), a rod (Wang and Kim, 1996; Oppenheimer and Dubowsky, 2003; Maragakis and Jennings, 1987; Khulief and Shabana, 1986) or a beam (Kahraman and Blankenship, 1997; Lin and Weng, 2001). It can be a movable element (Kahraman and Blankenship, 1997; Dubowsky and Freudenstein, 1971; Oppenheimer and Dubowsky, 2003; Wu and Thompson, 2004; Lin and Weng, 2001; Khulief and Shabana, 1986) or a fixed one (Peek and Wagar, 1955; Santos et al., 1991; Lee, 2004; Wang and Kim, 1996; Knudsen and Massih, 2000; Leine et al., 2002; Yigit et al., 1990; Maragakis and Jennings, 1987; Abdul Azeez and Vakakis, 1999; Johansson, 1997).

The present paper focuses on the impact system of a beam impacting against a rod-like stop. In the literatures, some researchers yielded simplified models in order to reduce mathematical complexity. Bishop et al. (1996) adopted a single-degree-of-freedom model and Newton's restitutive factor to analyze the experimental results of a flexible beam impacting a rod repeatedly. Fegelman and Grosh (2002), instead, examined the experimental impact behavior of a loosely fixed component in an automobile seat-belt retractor by a one-degree-of-freedom and a multi-degree-of-freedom model. Maragakis and Jennings (1987) estimated the rigid body motions of a skew bridge during earthquakes based on a rigid beam impacting a pier springs model. Santos et al. (1991) proposed the model of a three-degree-of-freedom beam and a rigid seat to simulate suction and discharge valves impacting repeatedly against the seat in a hermetic reciprocating compressor. van de Vorst et al. (1996) suggested a four-mode beam model and applied it to finite element analysis to study a beam impacting two rods up and down. An experiment of a rod impacting a flexible beam was conducted by Wagg and Bishop (2002). They also suggested the model of a four-mode beam and a rigid rod in the simulation of the experimental results. Further, Fathi and Popplewell (1994) proposed the continuous beam model to calculate the repeated impact force between a valve and a seat. Experiments of a flexible beam impacting rods repeatedly were made by Oppenheimer and Dubowsky (2003), Cusumano et al. (1994) and Wagg et al. (1999). More comprehensive modelling, consisting of both a continuous beam and rod, has been adopted by very few researchers. By the use of the beam Green's function and St. Venant rod theory, Wang and Kim (1996) studied repeated impact in a small, fractional horsepower compressor. Oppenheimer and Dubowsky (2003) applied beam and rod finite elements to predict impact-induced acoustic noise in Machine Systems. By using the three-dimensional finite element method, Wang and Kim (1997) investigated the impact behavior of a beam impacting a stop of three-dimensional configuration. If the rod is modeled as a spring, as was done by Fegelman and Grosh (2002), some referential works can be found, for example, in Johansson (1997) for a tube wear problem, Sauvé and Teper (1987) for a loosely support tube impact problem, Abdul Azeez and Vakakis (1999) for the impact taking place in rotor systems, Knudsen and Massih (2000) for the impact problem in heat exchangers, Ting et al. (1979) for component-support impacts, and Lo (1980) for relay impacts.

However, there are three main difficulties on the study of repeated impact of beam-rod systems and also other more common flexible structural systems. First, it is well known that impact takes place during short time and will generate transient wave propagation that includes many more high frequency wave modes. The one-degree-of-freedom and multi-degree-of- freedom models have not adapted to depict high frequency vibrations generated by repeated impact. In the view of the theory of transient wave propagation (Achenbach, 1973), the transient wave effect will be strong if the impact duration is in a same magnitude as the time period required by the wave to travel across the whole component. The flexible waves resulting from impacts will travel at much slower speeds than those of the longitudinal and shear waves, and the time period required become longer. In this case, the impact duration is more possible to be less than the time period. Thus promote stronger transient wave effects. The solution of transient wave propagations is difficult in mathematics, even for such components as a single beam and a rod (Achenbach, 1973). More difficult problems are encountered in impact systems where all of the impacting components are flexible. As our knowledge, few researches have been involved in the transient wave effect of repeated impact as Yin (1997), Yin and Wang (1999) and Wang and Kim (1996).

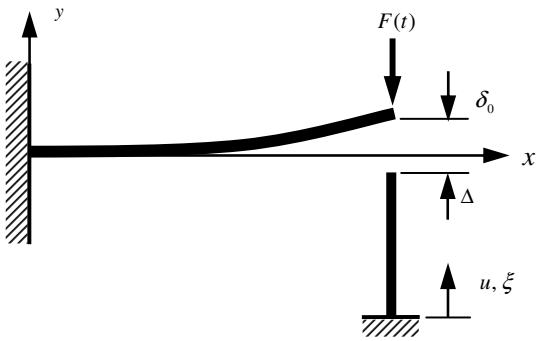

Fig. 1. Illustration of a beam and rod impact configuration.

Second, in the aforementioned researches, the impact force should be determined in advance, so as to obtain systematic responses. This is a difficult problem because the impact force can not be derived directly from the equation that comprises the unknown impact force and motions. The coupling effect is strong and non-linear, as discussed by Johansson (1997). Usually, time discretization methods have to be applied for obtaining the impact force by the iterative techniques, as shown in example references (Wang and Kim, 1996, 1997; Knudsen and Massih, 2000; Fathi and Popplewell, 1994; Johansson, 1997; Sauvé and Teper, 1987; Ting et al., 1979; Lo, 1980). Wang and Kim (1996) showed numerically that the estimation of impact force diverges in the time-discretization method, for example, the magnitude of the impact force almost diverges to infinity as time-step size approaches zero. The divergence might mean that the time-step size can not be chosen as small as desired and some empirical time increment sizes (rough time increment) should be used. Such a rough time gridding and its resultant error that will accumulate as the number of impacts increases will make the repeated-impact problem to be solved hardly, so that it is difficult to observe reliably the long-term vibratory behavior of a repeated-impact system.

The third difficult is reliability of long-term systematic dynamics with the less exact determinations of impact force and neglecting high frequency modes. As discussed by Paoli (2001), the complex dynamics of repeated-impact problems are sensitive to initial data and parameters and show chaotic behavior that may occur even for low-dimensional systems, see, for example, Moore et al. (1995) and Shaw and Holmes (1983). Hence, the high frequency modes and determination of repeated-impact force will play more important influence on non-linear dynamics of repeated-impact systems.

Therefore, it is significant to develop solving techniques to take account to the transient impact-induced wave effect, at least the high vibrational modes, and to provide more reliable and exact determinations of impact forces, so as to enable more exact and reliable investigations to be undertaken, and to be applicable for verifying the dynamics results obtained by low-degree-of-freedom models.

The objective of this research is to develop an approach for achieving a more exact and reliable analysis for the repeated-impact problem of a flexible impact system, i.e., the repeated impact of a beam against a rod. A schematic diagram of the proposed system is presented in Fig. 1. The solution, considering transient impact-induced wave propagations, is obtained in Section 2 by the use of the expansion of transient wave functions in a series of Eigenfunctions (wave modes). Section 2 will present a reliable and convenient method for determining impact forces. The dependence of the convergence of the solution on the time-step size and the truncation term number of wave modes selected is given numerically in Section 3. Also, several transient phenomena are shown in Section 3. Numerical investigation of the non-linearity of the long-term systematic responses involving impact-induced wave propagations will be performed and documented in later investigations.

2. Formulation

2.1. Model and natural frequencies

As shown in Fig. 1, a cantilever beam of length x_0, cross-section A, Young's modulus E, area moment of inertia I, mass density ρ and initial uplift δ_0 at the free end, is clamped at one end and a dynamic force

$F(t)$ applied at the beam tip. The beam impacts a rod of length l, cross-section A_s, Young's modulus E_s and mass density ρ_s. There is a gap Δ between the balance positions of the beam and the rod. The impact surface is considered planar and frictionless, and there is no plastic deformation of the contact surfaces due to impact.

The beam is assumed to be the Bernoulli–Euler beam and the rod to be a St. Venant rod having equations of motion described by:

$$a^2 \frac{\partial^4 y(x,t)}{\partial x^4} + \frac{\partial^2 y(x,t)}{\partial t^2} = 0 \tag{1}$$

$$\frac{\partial^2 u(\xi,t)}{\partial \xi^2} = \frac{1}{c^2} \frac{\partial^2 u(\xi,t)}{\partial t^2} \tag{2}$$

In these equations, $y(x,t)$ is the beam deflection, $u(\xi,t)$ is the longitudinal displacement of the rod. a is the coefficient related to the beam flexural wave speed and c is the rod phase speed given, respectively, by:

$$a = \sqrt{\frac{EI}{\rho A}} \quad \text{and} \quad c = \sqrt{\frac{E_s}{\rho_s}} \tag{3}$$

Here, the Bernoulli–Euler beam theory does not consider the longitudinal waves and the St. Venant rod theory merely consider the longitudinal waves, so that the beam and rod need to be slender. Also, external damping and contact damping are not included in the model.

The beam has two different sets of boundary conditions when the beam is in contact or out of contact with the rod. For the in-contact case, the boundary conditions are:

$$\begin{aligned} &y(0,t) = 0, \quad \frac{\partial y(0,t)}{\partial x} = 0, \quad M(x_0,t) = EI \frac{\partial^2 y(x_0,t)}{\partial x^2} = 0 \\ &Q(x_0,t) = EI \frac{\partial^3 y(x_0,t)}{\partial x^3} = -E_s A_s \frac{\partial u(l,t)}{\partial \xi} - F(t) \\ &y(x_0,t) = u(l,t) + \Delta, \quad u(0,t) = 0 \end{aligned} \tag{4}$$

in which $M(x,t)$ and $Q(x,t)$ are the beam bending moment and shearing force, respectively. The fourth term is the shearing force continuity condition, i.e., the negative shearing force at the end of the beam is equal to the sum of the applied force and the reaction force of the rod tip. The fifth term is the displacement continuity conditions. In this case, the beam and rod vibrate together at the frequencies ω_m from the following transcendental frequency equation, which will be solved in Section 2.2:

$$\begin{aligned} &E_s A_s k_{rm} \cos k_{rm} l (\sin k_{bm} x_0 chk_{bm} x_0 - \cos k_{bm} x_0 shk_{bm} x_0) + EIk_{bm}^3 \sin k_{rm} l (1 + \cos k_{bm} x_0 chk_{bm} x_0) = 0, k_{rm} \\ &\quad = \omega_m / c, \quad k_{bm} = \sqrt{\omega_m / a} \end{aligned} \tag{5}$$

For the out-of-contact case, the beam and rod vibrate separately at two different sets of natural frequencies ω_{bn} and ω_{rn}, respectively. The beam boundary conditions are identical in the first three conditions and another condition can be derived from the fourth condition when the contact force disappears. One of the rod boundary conditions is as same as the sixth condition and an additional boundary is zero axial force at the rod tip. The beam natural frequencies can be obtained numerically from the well-known transcendental frequency equation in Timoshenko et al. (1974):

$$\cos k_{bn} x_0 chk_{bn} x_0 + 1 = 0, \quad k_{bn} = \sqrt{\omega_{bn} / a} \tag{6}$$

The rod frequencies have also a well-known analytical form (Timoshenko et al., 1974):

$$\omega_{rn} = k_{rn} c, \quad k_{rn} = \frac{(2n-1)}{2l} \pi \tag{7}$$

In frequency Eqs. (5)–(7), k_{bn}, k_{rn}, k_{mb} and k_{mr} are corresponding wave numbers. All of the frequencies obtained in both cases will be useful for the exact solutions of transient wave propagations in the present paper.

2.2. Solutions of transient wave propagations in the in-contact case

The problem of the repeated impact between the beam and the rod is complex due to impact-induced waves. Fast and frequent impact will generate strong transient wave effects irrespective of whether the beam and rod are in contact or out of contact. In both cases, the flexural waves travel along the beam, and the longitudinal waves travel along the rod. They will interact at the contact position during the in-contact case and result in complicated structural dynamic responses. In this section, the transient wave propagations are solved by the use of the expansion of transient wave functions in a series of Eigenfunctions (i.e., wave modes). The general description of the method can be obtained by reference to the well-known text by Eringen and Suhubi (1975), the review paper by Pao (1983) or a recent application by Yin and Yue (2002).

The essential form of the solutions contains two parts. For example, in the in-contact case, the beam deflection and rod longitudinal displacement are expressed as follows:

$$y(x,t) = y_s(x,t) + \sum_{m=1}^{\infty} Y_m(x) q_m(t) \tag{8a}$$

$$u(\xi,t) = u_s(\xi,t) + \sum_{m=1}^{\infty} U_m(x) q_m(t) \tag{8b}$$

The first part of these equations contains the quasi-static solution. The two quasi-static solutions together satisfy all boundary conditions (4), which latter are called inhomogeneous boundary conditions because there is non-zero traction acting on the beam tip:

$$y_s(x,t) = [y_{s1}F(t) + y_{s2}\Delta](3x^2x_0 - x^3) \tag{9a}$$

$$u_s(\xi,t) = [u_{s1}F(t) + u_{s2}\Delta]\xi \tag{9b}$$

$$y_{s1} = -\frac{l}{6EIl + 2E_sA_sx_0^3}, \quad y_{s2} = -\frac{E_sA_s}{6EIl + 2E_sA_sx_0^3}$$

$$u_{s1} = -\frac{x_0^3}{3EIl + E_sA_sx_0^3}, \quad u_{s2} = \frac{3EI}{3EIl + E_sA_sx_0^3}$$

The second part contains the dynamic part that is the summation of an infinite series of the product of the wave modes (for the beam, flexural wave modes $Y_m(x)$; for the rod, longitudinal wave mode $U_m(\xi)$) and time functions $q_m(t)$. The wave modes are governed by the Eigenvalue problem with the Eigenequations:

$$a^2\frac{d^4Y_m(x)}{dx^4} - \omega_m^2 Y_m(x) = 0 \tag{10a}$$

$$c^2\frac{d^2U_m(\xi)}{d\xi^2} + \omega_m^2 U_m(\xi) = 0 \tag{10b}$$

and homogenous boundary conditions:

$$\begin{aligned} &Y_m(0) = 0, \quad \frac{dY_m(0)}{dx} = 0, \quad EI\frac{d^2Y_m(x_0)}{dx^2} = 0 \\ &EI\frac{d^3Y_m(x_0)}{dx^3} = E_sA_s\frac{dU_m(l)}{d\xi}, \quad Y_m(x_0) = U_m(l) \\ &U_m(0) = 0 \end{aligned} \tag{11}$$

The flexural wave modes $Y_m(x)$ have four terms obtained from Eq. (10a) in sinusoidal, cosinoidal, exponentially sinusoidal and exponentially cosinoidal functions. The longitudinal wave modes obtained from Eq. (10b) have two terms in sinusoidal and cosinoidal functions. Substituting them into the homogenous conditions (11) can provide a set of linear algebraic equation in matrix form. The existence of non-trivial solutions leads to the determinant of the coefficient matrix being zero, which forms the beam-rod frequency Eq. (5). Provided the

explicit expression of the coefficient A_m is determined by the orthogonality relation (13), the expression of the Eigenfunctions can be given as the following:

$$Y_m(x) = M_{m2}A_m[\sin k_{bm}x - shk_{bm}x + M_{m1}(\cos k_{bm}x - chk_{bm}x)] \tag{12a}$$

$$U_m(\xi) = A_m \sin k_{rm}\xi \tag{12b}$$

$$M_{m1} = -\frac{\sin k_{bm}x_0 + shk_{bm}x_0}{\cos k_{bm}x_0 + chk_{bm}x_0}$$

$$M_{m2} = -\frac{E_sA_sk_{rm}\cos k_{rm}l(\cos k_{bm}x_0 + chk_{bm}x_0)}{2EIk_{bm}^3(1 + \cos k_{bm}x_0 chk_{bm}x_0)}$$

The flexural and longitudinal wave modes form an orthogonal set, which can be derived easily from the Eigenequations (10a and 10b) and the homogenous boundary conditions (11):

$$\int_0^l \rho_s U_i(\xi)U_j(\xi)A_s\mathrm{d}\xi + \int_0^{x_0} \rho Y_i(x)Y_j(x)A\mathrm{d}x = \delta_{ij} \tag{13}$$

Note that for a structure with different materials in more than one parts, the mass density should always be included in the orthogonal condition (see also in Yin and Yue, 2002).

The construction of the quasi-static part and the dynamic part make the real boundary conditions (5) be satisfied completely, but the equations of motion (1) and (2) need to be satisfied by further construction of the time functions $q_m(t)$. The way to do this is to substitute expressions (8a) and (8b) into the equations of motion, and use the orthogonal condition (13) again to obtain an ordinary time differential equation of the time functions:

$$\begin{aligned} &\ddot{q}_m(t) + \omega_m^2 q_m(t) = \ddot{\psi}_m(t) \\ &\psi_m(t) = -\int_0^l \rho_s u_s(\xi,t)U_m(\xi)A_s\mathrm{d}\xi - \int_0^{x_0} \rho y_s(x,t)Y_m(x)A\mathrm{d}x \end{aligned} \tag{14}$$

Using Laplace transforms, a formal solution is obtained as follows:

$$\begin{aligned} q_m(t) &= q_m(0)\cos\omega_m t + \frac{1}{\omega_m}\dot{q}_m(0)\sin\omega_m t + \frac{1}{\omega_m}\int_0^t \ddot{\psi}_m(\tau)\sin\omega_m(t-\tau)\mathrm{d}\tau \\ q_m(0) &= \int_0^l u_0(\xi)U_m(\xi)A_s\mathrm{d}\xi + \int_0^{x_0} y_0(x)Y_m(x)A\mathrm{d}x + \psi_m(0) \\ \dot{q}_m(0) &= \int_0^l \dot{u}_0(\xi)U_m(\xi)A_s\mathrm{d}\xi + \int_0^{x_0} \dot{y}_0(x)Y_m(x)A\mathrm{d}x + \dot{\psi}_m(0) \end{aligned} \tag{15}$$

in which $y_0(x)$ and $\dot{y}_0(x)$ are the initial deflection and velocity distributions along the beam, and $u_0(\xi)$ and $\dot{u}_0(\xi)$ are the initial displacement and velocity distributions along the rod.

2.3. Solutions of transient wave propagations in the out-of-contact case

The above procedure for the in-contact case can be applied more easily to the out-of-contact case in which the flexural wave and longitudinal travel independently. The deflection $y_b(x,t)$ and the longitudinal displacement $u_r(\xi,t)$ are divided into two parts:

$$y_b(x,t) = y_{bs}(x,t) + \sum_{n=1}^{\infty} Y_{bn}(x)q_{bn}(t) \tag{16}$$

$$u_r(\xi,t) = u_{rs}(\xi,t) + \sum_{n=1}^{\infty} U_{rn}(\xi)q_{rn}(t) \tag{17}$$

Their quasi-static parts, $y_{bs}(x,t)$ and $u_{rs}(\xi,t)$, and wave modes $Y_{bn}(x)$ and $U_{rn}(\xi)$ (see also Timoshenko et al., 1974) are, respectively:

$$y_{bs}(x,t) = -\frac{F(t)}{6EI}(3x^2x_0 - x^3) \tag{18}$$

$$u_{rs}(\xi,t) = 0 \tag{19}$$

$$Y_{bn}(x) = A_{bn}\{\sin k_{bn}x - shk_{bn}x + M_{bn}(\cos k_{bn}x - chk_{bn}x) \tag{20}$$

$$M_{bn} = -\frac{\sin k_{bn}x_0 + shk_{bn}x_0}{\cos k_{bn}x_0 + chk_{bn}x_0}, \quad A_{bn} = \frac{1}{\sqrt{M_{bn}^2 Ax_0}}$$

$$U_{rn}(\xi) = \sqrt{2/A_s l}\sin k_{rn}\xi \tag{21}$$

where $u_{rs}(\xi,t)$ is zero because no external force is applied on the rod when the beam and the rod are separate. The time functions, $q_{bn}(t)$ and $q_{rn}(t)$, and their initial values, q_{bn} (0), $q_{rn}(0)$, $\dot{q}_{bn}(0)$ and $\dot{q}_{rn}(0)$, have the same forms as that of $q_m(t)$, $q_m(0)$ and $\dot{q}_m(0)$, but they have their own frequencies, ω_{bn} and ω_{rn}, and initial displacement and velocity distributions, y_{b0} (x), $\dot{y}_{b0}(x)$, $u_{r0}(\xi)$ and $\dot{u}_{r0}(\xi)$, and their own integral parts.

Note that the solutions (8), (16) and (17) are constructed for solving the propagations of transient wave. However, the normal vibrational solutions (Timoshenko et al., 1974) are different and usually are applied to the vibrational analyses of beam and rod, but can not be applied to show the traveling of a transient wave. The main difference is that in the normal vibrational solutions, the quasi-static displacement terms as shown in solutions (8) are absent. Such an absence allows the solutions to satisfy merely the homogenous boundary with zero traction $F(t)$. This is because of the left dynamic part in the solutions is the summation of the wave modes $Y(x)$ or $U(\xi)$. These wave modes satisfy only the homogeneous boundary conditions, for example, the conditions (11). Hence, the absence of the quasi-static displacement term means that the normal vibrational solutions can not satisfy the real stress boundary (4) with non-zero traction. It will strongly influence the determination of impact force.

Similar discussions of the comparisons of the solutions for the propagations of transient waves in multilayered hollow cylinders can be seen in Yin and Yue (2002). The convergence of the present solutions of transient wave propagation can be discussed as well in a theoretical scheme similar to that shown in Yin and Yue (2002).

2.4. Impact force determination

During the period of the impact process, the impact force $P(t)$ is generated between the tips of the beam and the rod. The time discretization method to solve impact forces may be described. If the beam motion is expressed by $\bar{y}(x,t,P(t))$ and the rod motion is expressed by $\bar{u}(\xi,t,P(t))$, then the equation used by the time discretization method is:

$$\bar{y}(x,t,P(t))|_{x=x_0} = \bar{u}(\xi,t,P(t))|_{\xi=l} \tag{22}$$

In Eq. (22), the impact force and the beam and rod motions are strongly coupled. To solve the impact force, the Eq. (22) should be discretized in time at first. Then, the balance of the Eq. (22) reaches by searching the impact force by the use of the iterative techniques. As discussed in Section 1, to obtain the impact force by the time discretization method might not be an easy task and might produce lower numerical precision than would be anticipated. The coupling of the impact force and motions can be uncoupled only when the impact force can be expressed as an explicit function of the relative motion between the two impact bodies. If one of the impact bodies can be modeled as a linear/non-linear spring, the uncoupling can be obtained (Metallidis and Natsiavas, 2000). If the uncoupling can not be obtained, the time discretization method should be applied (Wang and Kim, 1996).

In the present study, the impact force is solved by the solutions of the transient wave response, and the time discretization method is therefore avoided. It might be called the transient wave response method. There are two main steps in calculating the impact force by such a method. First, the transient wave propagations in the in-contact case are solved as depicted in Section 2.2. Then, the internal forces, the bending shearing force at the beam tip and the internal pressure at the rod end, are obtained and expressed in terms of the solution of the transient wave propagations. These two forms of internal force can be used to express the impact force.

The impact force is either the bending shearing force minus the external force at the beam tip, or the internal pressure along the axis of the rod at the rod end:

$$-P(t) = -EI\frac{\partial^3 y(x_0,t)}{\partial x^3} - F(t) \quad \text{or} \quad -P(t) = E_s A_s \frac{\partial u(l,t)}{\partial \xi} \tag{23}$$

It is found that using the present method to determine the impact force may have some of the following advantages:

1. The well-established theories for the transient wave propagation in the beam and the rod in Sections 2.2 and 2.3 make the determination of the impact forces from the expressions (23) more reliable.
2. The motions of the beam and rod do not rely upon an *a priori* solution for the impact force.
3. Strong non-linear coupling between the motions and the impact force is avoided in the steps of the solution, although such a coupling effect is an inherent characteristic and appears in almost all impact systems.
4. Other systematic responses can be calculated individually without *a priori* calculation of the impact force.
5. There is no theoretical limitation of time-step size, except for those of computer capacity and computer time costs.

A similar method has been used successfully in the authors' previous papers on the multiple-impact problems of two coaxial hollow cylinders (see Yin, 1997 and Yin and Wang, 1999). It should be noted that the precision of the calculation of the impact force has an influence on the estimation of the time of termination of an impact process.

2.5. Solution of the repeated-impact problem

In considering the propagation of transient waves, the repeated-impact event is assumed to consist of three phases:

1. Pre-impact. During this phase, the beam vibrates and the rod rests.
2. Impact. During this phase, the beam is in contact with the rod, and vibrates together with the rod.
3. Separation. The beam is out of contact with the rod. The beam and rod vibrate separately. The rod vibrates due the remaining wave motions.

The impact and separation phases continue one-by-one. Despite the pre-impact phase, every phase has its own initial value conditions, i.e., the initial displacement and velocity distributions, which are changed from the previous phase and are the remaining distributions at the moment of the ending of the previous phase. In each phase, the transient responses can be solved from the theories in the in-contact case or out-of-contact case given in Sections 2.2 and 2.3, but the time variable should be adjusted so as to start at the initial time of its phase.

The initial displacement and velocity distributions in each of the three phases can be expressed in analytical form, which makes the solution more reliable.

For the pre-impact phase, they are:

$$y_{b0}(x) = \delta_0(1.5x^2x_0^{-2} - 0.5x^3x_0^{-3}), \quad \dot{y}_{b0}(x) = 0 \tag{24}$$

For the impact phase, they are:

$$\begin{aligned} y_0(x) &= y_{bs}(x,t_e) + \sum_{n=1}^{\infty} Y_{bn}(x) q_{bn}(t_e), \quad \dot{y}_0(x) = \dot{y}_{bs}(x,t_e) + \sum_{n=1}^{\infty} Y_{bn}(x)\dot{q}_{bn}(t_e) \\ u_0(\xi) &= u_{rs}(\xi,t_e) + \sum_{n=1}^{\infty} U_{rn}(\xi) q_{rn}(t_e), \quad \dot{u}_0(\xi) = \dot{u}_{rs}(\xi,t_e) + \sum_{n=1}^{\infty} U_{rn}(\xi)\dot{q}_{rn}(t_e) \end{aligned} \tag{25}$$

in which the time t_e is the time of termination of the previous phase. Substituting these expressions into Eq. (15), the analytical forms of $q_m(0)$ and $\dot{q}_m(0)$ can be obtained without difficulty by integrating each term.

For the separation phase, they are:

$$y_{b0}(x) = y_s(x, t_e) + \sum_{m=1}^{\infty} Y_m(x) q_m(t_e), \quad \dot{y}_{b0}(x) = \dot{y}_s(x, t_e) + \sum_{m=1}^{\infty} Y_m(x) \dot{q}_m(t_e) \tag{26}$$

$$u_{r0}(\xi) = u_s(\xi, t_e) + \sum_{m=1}^{\infty} U_m(x) q_m(t_e), \quad \dot{u}_{r0}(\xi) = \dot{u}_s(\xi, t_e) + \sum_{m=1}^{\infty} U_m(x) \dot{q}_m(t_e) \tag{27}$$

and the analytical forms of $q_{bn}(0)$, $q_{rn}(0)$, $\dot{q}_{bn}(0)$ and $\dot{q}_{rn}(0)$ can be obtained similarly.

The remaining determination is the time of initiation of each phase. As one phase ends the next phase begins, so that the termination time t_e of the previous phase is the initiation time of the present phase. The following in-contact condition (28) and out-of-contact condition (29) are used to determine the time t_e numerically:

$$U(t_e) = [u_r(l, t_e) - \Delta] - y_b(x_0, t_e) = 0, \quad \frac{\mathrm{d}U(t_e)}{\mathrm{d}t} \geqslant 0 \tag{28}$$

$$P(t) = 0, \quad \frac{\mathrm{d}P(t)}{\mathrm{d}t} \leqslant 0 \tag{29}$$

During the out-of-contact phase, the in-contact condition (28) means that when the gap between the beam tip and the rod tip $U(t)$ becomes zero and $\frac{\mathrm{d}U(t)}{\mathrm{d}t} \geqslant 0$, a new impact takes place. If $U(t) = 0$ and $\frac{\mathrm{d}U(t)}{\mathrm{d}t} < 0$, the gap will become positive value immediately and a new impact will not take place, or in other words, a "graze impact" with zero contact time occurs. During the in-contact phase, the out-of-contact condition (29) means that when the impact force $P(t)$ becomes zero and $\frac{\mathrm{d}P(t)}{\mathrm{d}t} \leqslant 0$, a new separation takes place, and then no impact force exists. But, for the simplicity in the plot of the impact force, the impact force can be assumed to be zero during the next out-of-contact phase. If $P(t) = 0$ and $\frac{\mathrm{d}P(t)}{\mathrm{d}t} > 0$, the impact force will become positive value immediately and no separation take place, or in other words, a "graze separation" with zero separation time occurs.

The forms of both conditions are as same as those by Yin (1997), Yin and Wang (1999) and Luo and Hanagud (1998). The in-contact condition is expressed by the motions, and the out-contact conditions is expressed by the impact force. As discussed by Luo and Hanagud (1998), when both conditions are expressed by the motions, the incorrect results of tensile contact force might occur sometimes.

The application of the present analytical method by substituting the solutions of the transient wave propagations in the in-contact case and out-of-contact, and the impact expression (23) into the Eqs. (28) and (29), results in the transcendental equations for determining the time which depends only upon the known structural and material properties. Such equations for solving the contact and separation time may be obtained with other methods such as that for one of the impact bodies modeled as a spring (Metallidis and Natsiavas, 2000). The considerations were, however, not given to the impact of two continuous bodies, except that reported by the first author of this paper (Yin, 1997; Yin and Wang, 1999).

The analytical expression of the solutions of Transient Wave Propagations in both in-contact and out-of-contact cases, explicit expression of the impact and the transcendental equations for determining the contact and separation time, make the solution of the repeated impact problem easier to be implemented by a computer program, and it also enable computing time saving.

3. Numerical results

To show some examples in this Section, the properties of the rod and beam under study are chosen. For the rod: $l = 0.01$ m, $A_s = 0.00052$ m (width) $\times$ 0.000104 m (thickness), $\rho_s = 7500$ kg/m^3, and Young's modulus $E_s = 200 \times 10^9$ N/m^2, and for the beam: $x_0 = 0.010617$ m, $A = 0.0254$ m (width) $\times$ 0.051 m (thickness), $I = 2.808 \times 10^{-7}$ m^4, $\rho = 7500$ kg/m^3, and Young's modulus $E = 145.04 \times 10^9$ N/m^2. They are selected, for comparisons purposes, as the same as those given by Lo (1980) and Wang and Kim (1996) modeling a small, fractional horsepower compressor.

3.1. Impact-induced waves

Fig. 2 shows the traveling of an impact-induced transient wave by the flexural deflections of the beam at different time instants after initial impact. For a beam with initial uplift of $\delta_0 = 0.01$ m and a zero gap $\Delta = 0$ between the beam and the rod, the initial impact starts at 7.64833 ms, after which the transient impact-induced flexural waves originate. The velocity wave response and bending moment wave response of the middle section of the beam are shown in Fig. 3. The initial impact force sub-structure is shown in Fig. 4. Compared to the beam deflection without impact shown as a dashed line in Fig. 2, the later deflections shown in solid lines are distorted, obviously by the flexural waves excited by the initial impact.

In Fig. 2, the dispersion characteristics of the beam flexural waves can generate different wave fronts according their wave mode frequencies. The first three impact-induced wave fronts have clear arrivals at non-dimensional positions 0.7538, 0.4020 and 0.2181, respectively, at the instant $t = 7.67908$ ms (thick solid line). Simultaneously, the fourth wave front has been reflected from the clamped end, travels in the opposite direction, and arrives clearly at the position 0.09. Unlike the impact-induced, non-dispersive, compressive waves traveling along the rod (not shown here), the impact-induced flexural waves traveling along the beam are dispersive waves. They travel in a more complex traveling manner, with the wave phase speed dependent on the excitation wave frequencies, i.e., $\sqrt{a\omega}$.

From the arriving positions and instants, the first four frequencies of the initial impact-induced wave modes can be estimated from the Fig. 2: these are 168510.0, 994042.2, 1699208.0 and 3302153 rad/s, respectively. The corresponding convergence number of the beam-rod modes required to well-matched these results are 18, 48, 65 and 97, respectively. The comparison means that at least more than 100 modes are required in the solution. Hence, the number of the wave modes used by the four-mode models might be too few to predict the wave propagations and the impact-contact force in the beam-stop system. In Fig. 2, the number of wave modes N is chosen to be 2000 for the purposes of comparison, but for normal calculations the 200 wave modes are enough to obtain reliable numerical results.

In Fig. 3, the middle of the beam has a strong response to the impacts. During the pre-impact phase, the beam vibrates with low frequencies and low amplitude. After the first impact at 7.64833 ms, the middle of the beam cannot vibrate quickly until the first impact-induced wave arrives. The responses of the velocity and the bending moment show the beam vibrates with either high frequencies or high amplitudes. The first separation occurs within a small interval after the first impact. During the first separation phase, the beam still vibrates with high frequencies.

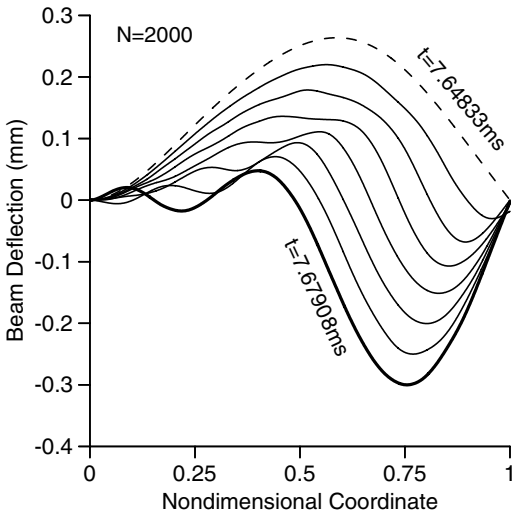

Fig. 2. Flexural wave propagation along the beam.

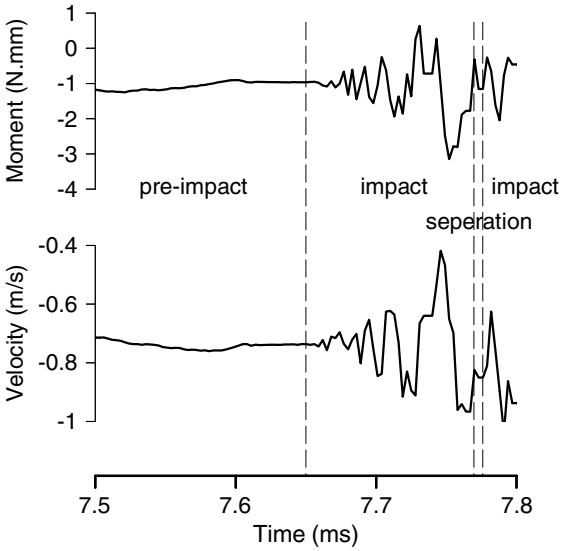

Fig. 3. Velocity wave and bending moment wave response at the middle of the beam.

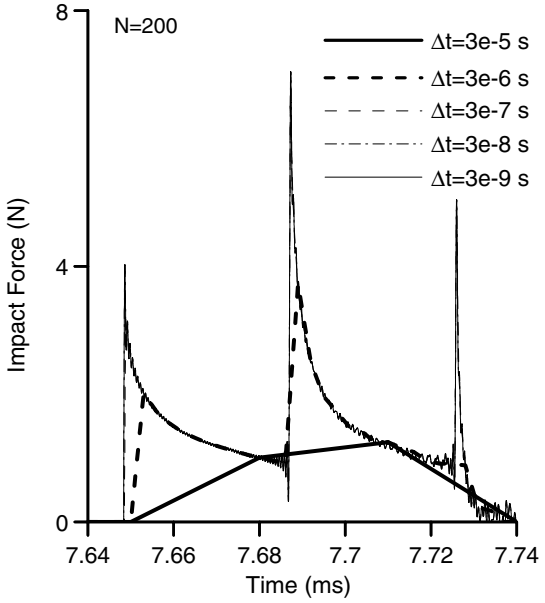

Fig. 4. Initial impact force history by different time-step increments.

The numerical results in Figs. 2 and 3 show that the traveling wave is indeed induced by impacts, and the method presented in this paper can capture the traveling behaviors of such an impact-induced wave. The numerical results in Fig. 3 also show that the impacts can result in high frequency and high amplitude vibrational responses.

3.2. Time-step increment, convergence

To capture sub-impact processes and consider high frequency transient responses, small time-step increments are required in numerical calculations. Until now, convergence has not been proven for the time discretization methods usually applied to determine impact forces in impact systems. The selection of small time-step

increments has been shown not to be suitable for some of them. For example, Wang and Kim (1996) have shown numerically that the method will give infinite magnitudes of impact force when the time-step increment tends to zero. Also, still no theory has been provided to prove their convergence (see the statement in Paoli, 2001). The present method given in this paper is based on the Bernoulli–Euler beam theory and the St. Venant rod theory in elasticity. Except for the numerical solving of the beam natural frequencies, beam-rod natural frequencies, impact and separation times, the other features are expressed in analytical functions. Hence, more exact numerical results might be gained easily.

To study the convergence of the present method with different time-step increments, Fig. 4 gives a detailed numerical comparison of the initial impact force histories in an incremental series arranged such that each subsequent increment is one tenth that of the previous one. For the time-step increment of 3e−5 s, the time history obtained is nearly a smooth curve without sharp peaks. It loses obviously some important information that represents the transient characteristics. For the size 3e−6 s, these characteristics have been secured successfully. The next three time-step increments have the same functions, and provide nearly the same time histories. The last increment 3e−9 s is only one thousandth of the size 3e−6 s. Fig. 4 shows clearly that no singularity exists in calculating the magnitudes of the impact force. Fig. 4 shows numerically not only the convergence of the force peaks, but also the whole time history. Hence, in the present method, the time increment can be selected as small as 3e−9 s.

Another convergence problem to be considered is the convergence of the number of wave modes, the truncation term numbers in the wave mode series in the solving expressions. To study the convergence, the time histories of impact force are calculated for $N = 5$, 10, 50, 100, 200, 400, 1000 and 2000. Fig. 5 shows five of them. Fig. 5 is a 3D plot with the x-axis denotes the time, y-axis the impact force and z-axis the number of modes.

When $N = 5$, usually selected in many other researches, the result can only give a very rough force structure that does not show sub-impact processes. The numerical result for $N = 10$ begins to exhibit some sub-impact process roughly, while that given by $N = 50$ can show sub-impact processes distinctly. An explanation may be that fifty wave modes have covered the first two impact-induced wave frequencies that influence the beam transient deflection substantially, as illustrated in Fig. 2. For $N = 100$, all of the first four impact-induced frequencies have been covered, which may be the reason why its time history is almost the same as that obtained when selecting two thousand wave modes, $N = 2000$. Time histories calculated for $N = 200$, 400 and 1000 have not been shown, because they are the same as the results for $N = 100$ and $N = 2000$. Fig. 5 also shows numer-

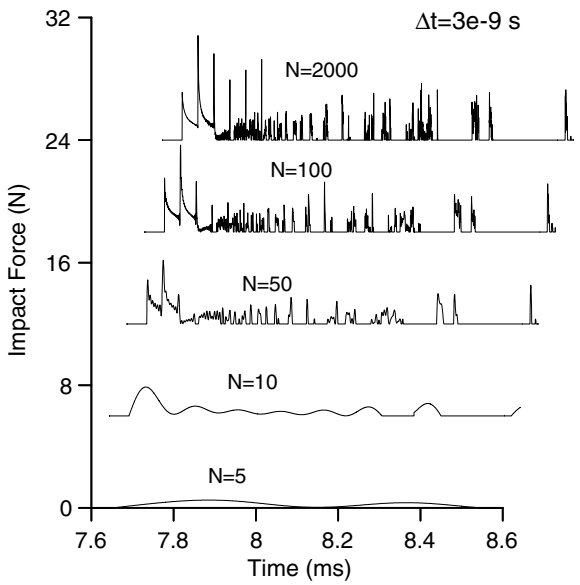

Fig. 5. Serial impact time histories calculated by different number of wave modes.

ically the convergence for the history of repeated impact forces. Therefore, larger modes can be used, and wave traveling phenomenon can then be displayed.

The convergence shown in Figs. 4 and 5 is helpful especially for the numerical modeling of impact systems, in which inherent parameter sensitivity is always encountered. In addition, a similar theoretical explanation for the convergence of the number of wave modes can be found in the paper by Yin and Yue (2002).

3.3. Long-term responses and chatter phenomenon

Considering the long-term responses of an impact system, the transient impact-induced wave effects are still strong because of repeated impacts without stopping, as shown in Fig. 6. An unsuitable method can accumulate calculation errors step-by-step more seriously, and may result in the unreal modeling of system responses. The convergence on the time-step size and the number of wave modes is significant for the long-term responses. The convergence shown numerically in Section 3.2 may mean that the present method is suitable for the calculation of the long-term responses of beam-stop impact systems and investigating their nonlinearity.

Fig. 6 shows clearly the long-term impact force and beam deflection responses, whilst Fig. 2 shows a detailed part. In both of these figures, the beam tip is subjected to a harmonic external force $F(t) = 0.01\sin(50t)$ with amplitude 0.01 N and circular excitation frequency 50 rad/s, the initial beam uplift δ_0 is zero and the gap Δ is also zero. Some results can be obtained:

1. The maximum impact force is 0.8076 N. The peak values of sub-impact force are frequently over 0.1 N. If the beam is assumed never to move away from the rod, the contact force is 0.01004 N, which can be found in the initial impact phase during the time from 0 to 0.06274 s. Hence, the impact force can easily be more than ten times the contact force. This is a well-known characteristic of repeated impact systems found in numerical simulations and experiments by many other researchers (Goldsmith, 1960; Dubowsky and Freudenstein, 1971).
2. There are many sub-impact phases, see also Figs. 4–6.
3. Sub-impacts take place, concentrated in the time intervals when the excitation is push force. If push and lift forces are designed, for example, to close and open the valve reed in compressors, it can be considered that impact and closing is synchronous.

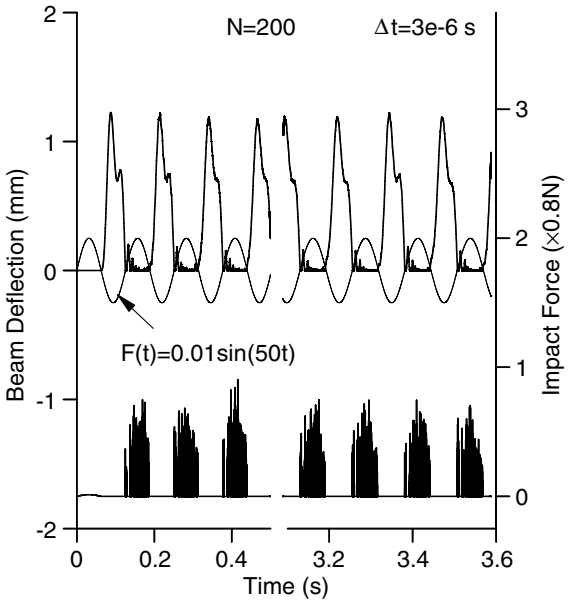

Fig. 6. Long-term responses of the beam.

4. The synchronous phenomenon shown in Fig. 6 is not an ideal one. The detailed part shown in Fig. 7 illustrates that there are many sub-impacts, although the corresponding impact zone in Fig. 6 looks like a single impact process. The sub-impacts always cause sub-bounds of the beam, so that the closing might not be performed completely.
5. During a period of excitation, the impact zone contains a quick succession of sub-impacts. This phenomenon is referred to as "chatter" and is usually accompanied with so-called "sticking motion". Such sticking motion can be observed in Fig. 7, in which the beam impacts and bounds continuously and seems to eventually rest on the rod.

It was thought that sticking motion could not be easily detected experimentally due to the limitations in experimental sampling rate (Wagg and Bishop, 2002), and that special treatments are required to be developed to simulate the sticking motion numerically. However, the resulting sticking motion shown in Fig. 7 is obtained without any additional treatment, just as same as the solution process performed for Figs. 2–6.

3.4. Asynchronous impact and contact loss

An impact taking place during the push phase of the force excitation is called as a Synchronous impact. An impacts taking place during the lift phase of the force excitation is, however, defined as an Asynchronous impact. If an impact can take place during either the push phase or the lift phase of the force excitation, it is then called as a Non-synchronous impact. Under some excitation frequencies, a non-synchronous impact phenomenon is observed. It will be harmful for an impact system, if the closing action is designed to be controlled by push force. Fig. 8 shows an interesting extreme example, an Asynchronous impact phenomenon, in which all the sub-impacts after the first period are observed under lift force excitation.

Another transient phenomenon is impact loss. The phenomenon can be defined here as the absence of impact during some periods of excitation. Fig. 9 shows part of long-term impact force and beam deflection responses under high frequency excitation $F(t) = 0.01\sin(820t)$. There are merely three periods containing impact-contacts, whilst for seventeen other periods there is loss of impact. If the impact-contact is required to perform the closing action within some designed time interval, impact loss may make it impossible. As a prediction, high frequency excitation may generate more strong transient responses and cause irregular impact loss to occur more easily.

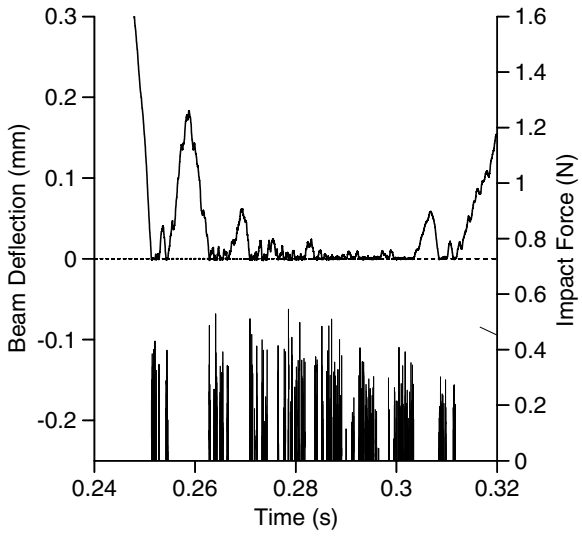

Fig. 7. The beam sticking motion.

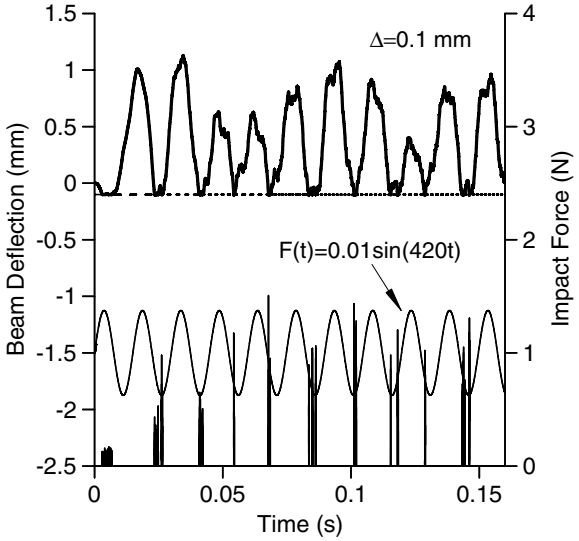

Fig. 8. Asynchronous impact-contact ($N = 200$, $\Delta t = 3e{-}6$ s).

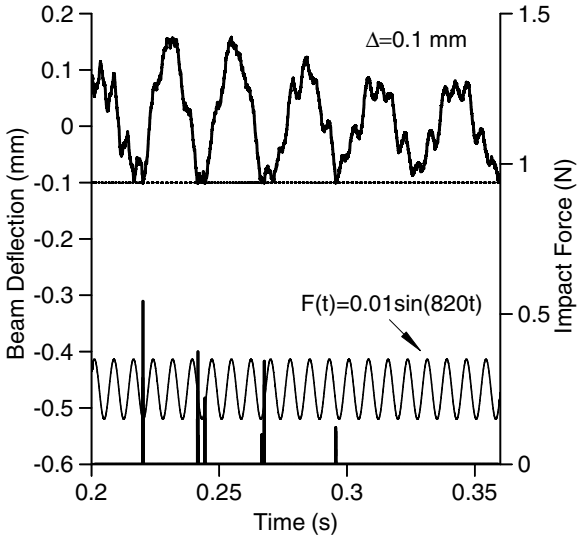

Fig. 9. Impact-contact loss ($N = 200$, $\Delta t = 3e{-}6$ s).

4. Conclusions

Many engineering systems involving repeated impact can be modeled as a beam impact against a rod. The model of the impact system of a beam repeatedly impacting against the rod by the use of the Bernoulli–Euler beam theory and St. Venent rod theory is a more exact continuous model, although these two elasticity theories still have some limitations. By the use of the expansion of transient wave functions in a series of Eigenfunctions, the exact solutions of transient wave propagations along the beam, rod and beam-rod frame provide a more reliable theoretical base. The exact and convenient solving method for impact force presented herein dramatically establishes another reliable base. Then well-built solutions of the repeated-impact problem can be expressed analytically, except for the requirements of four numerical solutions, i.e., the beam natural frequencies, the beam-rod frame natural frequencies, and the initial and terminal instants of each impact phase. The first two numerical solutions can be solved with sufficient precision due to the capacity of modern

computers. The later two numerical solutions can be solved with high precision, but there is a problem left due to the theoretical difficulty in capturing graze impacts at zero impact velocity. In fact, these graze impacts have zero time interval theoretically and the cautions regarding them can focus on very short impact phases. However, the convergence of time-step size and wave number selected, which have been numerically illustrated in the present paper, can greatly cut down the hazard coming from these very short impacts.

The convergence proven numerically herein is of foremost importance for long-term transient responses. It can ensure not only reliable and exact numerical results of impact force, displacement and other systematic responses that are influenced strongly the impact-induced wave propagations, but also the reliable observation of system non-linearity that will be discussed later.

The present study has shown some important physical phenomena: the propagation of transient impact-induced waves, the sub-impact phase, high impact force, long-term impact motion, chatter, sticking motion, synchronous impact, non-synchronous impact (including asynchronous impact) and impact loss. There might be many other phenomena not shown, some of which may have not have been observed ever before. However, there is no theoretical or methodological difficulty in the application of the present method to make the observation of these phenomena. For some phenomena, such as sticking motion, to detect which there is some difficulty in experiments, the present method can be used as a supplementary method in theoretical and numerical analysis. For many other simpler models used for the analysis of impact systems, the present method can provide more reliable results for examinations and comparisons. Such work can also be done for numerical techniques such as the finite element methods.

Acknowledgments

The work reported was sponsored partially by National Basic Science Project a2620060249, Nanjing University of Science and Technology and University of Strathlcyde, these supports are gratefully acknowledged.

References

Abdul Azeez, M.F., Vakakis, A.F., 1999. Numerical and experimental analysis of a continuous overhung rotor undergoing vibro-impacts. Int. J. Non-linear Mech. 34 (3), 415–435.

Achenbach, J.D., 1973. Wave Propagation in Elastic Solids. North Holland, Amsterdam.

Babitsky, V.I., 1978. Theory of Vibro-Impact Systems and Applications. Springer, Berlin, Revised Translation from Russian, Moscow, Nauka.

Bishop, S.R., Thompson, M.G., Foale, S., 1996. Prediction of period-1 impact in a driven beam. Proc. R. Soc. Lond. A 452 (1954), 2579–2592.

Cusumano, J.P., Sharkady, M.T., Kimble, B.W., 1994. Experimental measurements of dimensionality and spatial coherence in the dynamics of a flexible-beam impact oscillator. Philos. Trans. R. Soc. Lond. A 347 (1683), 421–438.

Dubowsky, S., Freudenstein, F., 1971. Dynamic analysis of mechanical systems with clearances, Part 1: formation of dynamic mode, and Part 2: dynamic response. ASME J. Eng. Ind. 93B, 305–316.

Eringen, A.C., Suhubi, E.S., 1975. Elastodynamics. In: Linear Theory, vol. 2. Academic Press, New York.

Fathi, A., Popplewell, N., 1994. Improved approximations for a beam impacting a stop. J. Sound Vib. 170 (3), 365–375.

Fegelman, K.J.L., Grosh, K., 2002. Dynamics of a flexible beam contacting a linear spring at low frequency excitation: experiment and analysis. ASME J. Vibr. Acoust. 124 (2), 237–249.

Goldsmith, W., 1960. Impact: The Theory and Physical Behaviour of Colliding solids. Edward Arnold Ltd., London.

Johansson, L., 1997. Beam motion with unilateral contact constraints and wear of contact sites. ASME J. Press. Vessel Technol. 119 (1), 105–110.

Kahraman, A., Blankenship, G.W., 1997. Experiments on nonlinear dynamic behavior of an oscillator with clearance and periodically time-varying parameters. ASME J. Appl. Mech. 64 (1), 217–226.

Khulief, Y.A., Shabana, A.A., 1986. Dynamic analysis of a constrained system of rigid and flexible bodies with intermittent motion. ASME J. Mech., Transm. Autom. Des. 108, 38–45.

Knudsen, J., Massih, A.R., 2000. Vibro-impact dynamics of a periodically forced beam. ASME J. Press. Vessel Technol. 122 (2), 210–221.

Lee, K., 2004. Dynamic contact analysis for the valvetrain dynamics of an internal combustion engine by finite element techniques. Proc. Inst. Mech. Eng. Part D J. Automobile Eng. 218 (3), 353–358.

Leine, R.I., van Campen, D.H., Keultjes, W.J.G., 2002. Stick-slip whirl interaction in drillstring dynamics. ASME J. Vibr. Acoust. 124 (2), 209–220.

Lin, J.-H., Weng, C.-C., 2001. Probability analysis of seismic pounding of adjacent buildings. Earthquake Eng. Struct. Dyn. 30 (10), 1539–1557.

Lo, C.C., 1980. A cantilever beam chattering against a stop. J. Sound Vib. 69 (2), 245–255.

Luo, H., Hanagud, S., 1998. On the dynamics of vibration absorbers with motion-limiting stops. ASME J. Appl. Mech. 65 (1), 223–233.
Maragakis, E.A., Jennings, P.C., 1987. Analytical modals for the rigid body motions of skew bridges. Earthquake Eng. Struct. Dyn. 15 (8), 923–944.
Metallidis, P., Natsiavas, S., 2000. Vibration of a continuous system with clearance and motion constraints. Int. J. Non-linear Mech. 35 (4), 675–690.
Moore, J.J., Palazzolo, A.B., Gadangi, R., Nale, T.A., Klusman, S.A., Brown, G.V., Kascak, A.F., 1995. A forced response analysis and application of impact dampers to rotordynamic vibration suppression in a cryogenic environment. ASME J. Vibr. Acoust. 117 (3A), 300–310.
Oppenheimer, C.H., Dubowsky, S., 2003. A methodology for predicting impact-induced acoustic noise in machine systems. J. Sound Vib. 266 (5), 1025–1051.
Pao, Y.H., 1983. Elastic waves in solids. ASME J. Appl. Mech. 50 (4b), 1152–1164.
Paoli, L., 2001. Time discretization of vibro-impact. Philos. Trans. R. Soc. Lond. A 359 (1798), 2405–2428.
Peek Jr., R.L., Wagar, H.N., 1955. Switching Relay Design. D. Van Nostrand Co., Inc., Princeton, New Jersey.
de los Santos, M.A., Cardona, S., Sánchez-Reyes, J., 1991. A global simulation model for hermetic reciprocating compressor. ASME J. Vibr. Acoust. 113 (3), 395–400.
Sauvé, R.G., Teper, W.W., 1987. Impact simulation of process equipment tubes and support plates – a numerical algorithm. ASME J. Press. Vessel Technol. 109 (1), 70–79.
Shaw, S.W., Holmes, P.J., 1983. A periodically forced impact oscillator with large dissipation. ASME J. Appl. Mech. 50 (4a), 849–857.
Theodossiades, S., Natsiavas, S., 2001. Periodic and chaotic dynamics of motor-driven gear-pair systems with backlash. Chaos Solitons Fract. 12, 2427–2440.
Timoshenko, S., Young, D.H., Weaver, W. JR., 1974. Vibration Problems in Engineering. John Wiley, New York.
Ting, E.C., Chen, S.S., Wambsganss, M.W., 1979. Dynamics of component-support impact: an elastic analysis. Nucl. Eng. Des. 52 (1), 235–244.
van de Vorst, E.L.B., van Campen, D.H., de Kraker, A., 1996. Periodic solutions of a multi-DOF beam system with impact. J. Sound Vib. 192 (5), 913–925.
Wagg, D.J., Bishop, S.R., 2002. Application of non-smooth modelling techniques to the dynamics of a flexible impacting beam. J. Sound Vib. 256 (5), 803–820.
Wagg, D.J., Karpodinis, G., Bishop, S.R., 1999. An experimental study of the impulse response of a vibro-impacting cantilever beam. J. Sound Vib. 228 (2), 243–264.
Wang, C., Kim, J., 1996. New analysis method for a thin beam impacting against a stop based on the full continuous model. J. Sound Vib. 191 (5), 809–823.
Wang, C., Kim, J., 1997. The dynamic analysis of a thin beam impacting against a stop of general three-dimensional geometry. J. Sound Vib. 203 (2), 237–249.
Wu, T.X., Thompson, D.J., 2004. The effects of track non-linearity on wheel/rail impact. Proc. Inst. Mech. Eng. Part F: J. Rail Rapid Transit. 218 (1), 1–15.
Yigit, A.S., Ulsoy, A.G., Scott, R.A., 1990. Dynamics of a radically rotating beam with impact, Part 1: theoretical and computational model. ASME J. Vibr. Acoust. 112 (1), 65–70.
Yin, X.C., 1997. Multiple impacts of two concentric hollow cylinders with zero clearance. Int. J. Solids Struct. 34 (35–36), 4597–4616.
Yin, X.C., Wang, L.G., 1999. The effect of multiple impacts on the dynamics of an impact system. J. Sound Vib. 228 (5), 995–1015.
Yin, X.C., Yue, Z.Q., 2002. Transient plane-strain response of multilayered elastic cylinders to axisymmetric impulse. ASME J. Appl. Mech. 69 (6), 826–835.